

New Insights into the Negative Thermal Expansion: Direct Experimental Evidence for the “Guitar-String” Effect in Cubic ScF_3

Lei Hu,[†] Jun Chen,^{*,†} Andrea Sanson,[‡] Hui Wu,[§] Clara Guglieri Rodriguez,^{||} Luca Olivi,^{||} Yang Ren,[⊥] Longlong Fan,[†] Jinxia Deng,[†] and Xianran Xing^{*,†}

[†]Department of Physical Chemistry, University of Science and Technology Beijing, Beijing 100083, China

[‡]Department of Physics and Astronomy, University of Padova, Padova I-35131, Italy

[§]NIST Center for Neutron Research, National Institute of Standards and Technology, Gaithersburg, Maryland 20878, United States

^{||}Elettra Synchrotron, Basovizza, Trieste I-34149, Italy

[⊥]Argonne National Laboratory, X-ray Science Division, Argonne, Illinois 60439, United States

Supporting Information

ABSTRACT: The understanding of the negative thermal expansion (NTE) mechanism remains challenging but critical for the development of NTE materials. This study sheds light on NTE of ScF_3 , one of the most outstanding materials with NTE. The local dynamics of ScF_3 has been investigated by a combined analysis of synchrotron-based X-ray total scattering, extended X-ray absorption fine structure, and neutron powder diffraction. Very interestingly, we observe that (i) the Sc–F nearest-neighbor distance strongly expands with increasing temperature, while the Sc–Sc next-nearest-neighbor distance contracts, (ii) the thermal ellipsoids of relative vibrations between Sc–F nearest-neighbors are highly elongated in the direction perpendicular to the Sc–F bond, indicating that the Sc–F bond is much softer to bend than to stretch, and (iii) there is mainly dynamically transverse motion of fluorine atoms, rather than static shifts. These results are direct experimental evidence for the NTE mechanism, in which the rigid unit is not necessary for the occurrence of NTE, and the key role is played by the transverse thermal vibrations of fluorine atoms through the “guitar-string” effect.

In the last two decades, negative thermal expansion (NTE) has been found in various types of oxides,¹ alloys,² nitrides,³ fluorides,^{4,5} and so on. Considering that even subtle variations of the coefficient of thermal expansion (CTE) tend to crucially degrade the performance of components or devices in optical, electronic, and biomedical industries, NTE materials have significantly technological applications for the precious control of thermal expansion.⁶ It has been well-known that the understanding of the NTE mechanism is crucial not only for the design of new NTE materials but also for the control of CTE.⁷ However, the nature of NTE is complicated and remains challenging since it is entangled with some factors like low-frequency phonons and transverse motions,⁸ magnetic transitions and ferroelectricity,⁹ changes of the electronic configuration, etc.¹⁰

Most NTE compounds have a common structural feature of open frameworks, like ZrM_2O_8 compounds ($M = \text{W}$ or

Mo),^{1,11} cubic fluorides,^{4,5,12} cyanides,⁸ metal–organic frameworks¹³ and their derivatives. Rigid unit mode (RUM) model has been proposed and widely accepted to account for these frameworks’ exotic NTE characteristic. RUM model assumes that polyhedral building blocks, consisting of 3D networks, have negligible variance in shape and size, even when subjected to drastic temperature fluctuation.¹⁴ However, even for the prototype NTE compound ZrW_2O_8 , the NTE mechanism remains debated: ZrO_6 and WO_4 were postulated to be rigid based on the RUM model, and the correlated rocking motion of these polyhedra shrinks the lattice volume on heating;^{1,15} in contrast, the tent model claims that the displacement of WO_4 along $[111]$ crystal direction and the correlated motion of the three nearest ZrO_6 octahedra contributes to NTE;¹⁶ recent molecular dynamics (MD) study revealed a more flexible model with rigid nearest chemical bonds and tension effect.^{17a}

The nature of NTE materials could be elucidated if a simple crystal structure is available. Recently, a compelling counterpart, cubic scandium trifluoride (ScF_3 , space group $Pm\bar{3}m$) has been reported to exhibit an interesting isotropic NTE behavior.⁴ The striking feature of the crystal structure of ScF_3 is that it is simply composed of corner-shared ScF_6 octahedra. Such simple cubic structure enables us to clarify the NTE nature. Here we report, for the first time, the direct experimental evidence for the NTE mechanism of ScF_3 , obtained by a combined analysis of the pair distribution function (PDF) of synchrotron X-ray total scattering, extended X-ray absorption fine structure (EXAFS), and neutron powder diffraction (NPD). Specifically, the transverse vibrational motion of bridging F atoms plays a dominating role in NTE of ScF_3 through the so-called “tension” or “guitar-string” effect.

The lattice constant, a , extracted from structure refinement of our synchrotron X-ray diffraction (SXRD), X-ray PDF and NPD, contracts smoothly on heating over a large temperature interval (Figure 1). The average linear CTE, α_l , is $-3.1 \times 10^{-6} \text{ K}^{-1}$ in the temperature range 300–800 K, in a good agreement with the previous report by Greve et al.⁴

By considering only the temperature dependence of the lattice constant, one can obtain an unphysical shrinkage of the

Received: March 4, 2016

Published: June 23, 2016

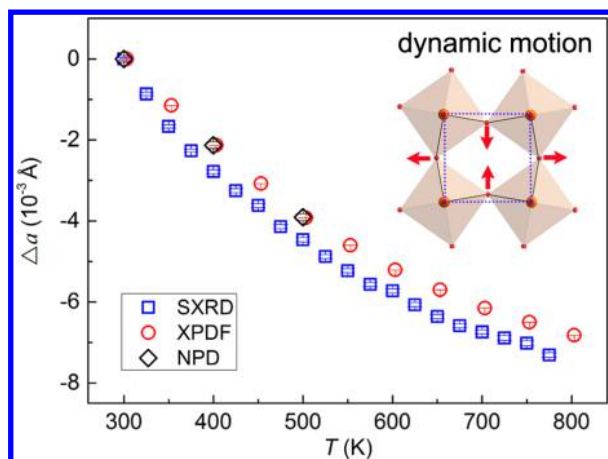


Figure 1. Temperature dependence of the relative lattice constant, Δa . The blue square, red circle and black diamond indicate refinement results extracted from high energy SXR, XP, and NP data, respectively. The inset shows the coupled rocking motion of ScF_6 octahedra. The red arrows reveal the dynamic motion of fluorine atoms.

“apparent” bond length under crystallographic symmetry constrains, such as that of the Sc–F bond ($a/2$). Therefore, we used here total scattering diffraction and EXAFS to measure the “true” bond length between neighboring atoms. The temperature dependence of the true Sc–F and Sc–Sc distances has been thus extracted (see Supporting Information for data analysis details). In contrast to the shrinkage of the apparent Sc–F distance ($\alpha_1 = -3.1 \times 10^{-6} \text{ K}^{-1}$) derived from the lattice constant, the true Sc–F bond expands steeply with increasing temperature (Figure 2a). The linear CTE is positive and as large as $+18.4 \times 10^{-6} \text{ K}^{-1}$, larger than the bond expansion coefficients observed in more flexible framework structures like ZrW_2O_8 ^{17a} or $\text{Zn}(\text{CN})_2$.^{8c} The large PTE of the real Sc–F bond length can be directly viewed from the temperature dependence of the Sc–F PDF peak between 1.75–2.25 Å of the $G(r)$ function (Figure 2b and 2c), where on heating the shift toward longer distances gives evidence of the considerable expansion of the real Sc–F bonds. On the contrary, the next-nearest neighbor Sc–Sc distance shrinks slowly with increasing temperature, with an average negative α_1 of $\sim -3.2 \times 10^{-6} \text{ K}^{-1}$, i.e., very similar to the lattice contraction. It needs to note that both XP and EXAFS results exhibit a good agreement. A recent density-functional MD simulations show that the calculated Sc–F bond also expands strongly with an approximate CTE of $+17.5 \times 10^{-6}/\text{K}$, 300–800 K (extracted from their data),^{17b} in accordance with the experimental results.

The correlation of vibrational motion plays a key role in the local behavior of NTE materials. First, before we understand the NTE mechanism of ScF_3 in light of transverse vibrational motion of fluorine, it needs to exclude the possibility of static shifts of fluorine away from the mean position, which could also bring the shrinkage of Sc–Sc distance. A disordered structure model with the F atoms distributing over (0.5, y , y) sites was employed to refine the NP data. However, the disordered one could not improve the refinement results (Figure S3), compared to the ideal cubic model with F atoms at (0.5, 0, 0) site. Besides, if the atomic displacement parameters of fluorine atoms in the ideal model are considered to calculate the Sc–F distance (Figure S4b), it also exhibits an apparent thermal expansion, consistent with the X-ray PDF result.

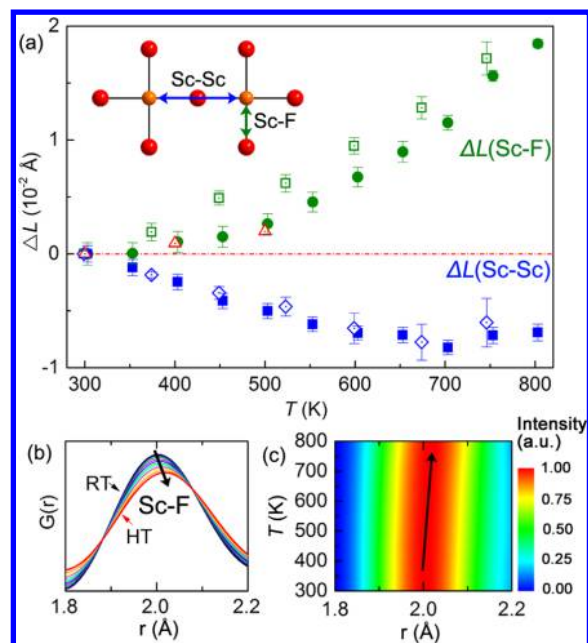


Figure 2. (a) True thermal expansion of the Sc–F and Sc–Sc bonds determined by XP (filled symbols) and EXAFS (open symbols). Green refers to the Sc–F bond and blue to the Sc–Sc atomic pair, shown in the inset. The red triangle indicates the Sc–F distance extracted from the NP data. (b) Temperature dependence of the first Sc–F shell (blue line at RT, red line at HT). (c) Contour plot of the normalized intensities of the Sc–F peak in $G(r)$ as a function of temperature.

Consequently, these results show that the dynamic vibration of fluorine atoms, instead of static shifts, is vital for the NTE behavior of ScF_3 .

In order to quantitatively investigate the correlated motion between selected pairs of neighboring atoms and have a complete description of the local dynamics, the atomic mean square relative displacement (MSRD) was extracted from the EXAFS data.¹⁸ Figure 3a shows the MSRD parallel to the bond direction of both Sc–F and Sc–Sc atomic pairs. The temperature dependence of the MSRD can be utilized to estimate the stiffness of the chemical bonds, which is represented by the effective force constant, k , obtained from the correlated Einstein model fit.¹⁸ The corresponding effective “bond-stretching” force constant k_{\parallel} for the Sc–F and Sc–Sc chemical bonds are about 9.38(7) and 6.55(24) $\text{eV}/\text{Å}^2$ (Table S1), respectively. It is worth noting that the Sc–F bond is stiffer than the nearest-neighbor bonds of some typical NTE, like Ag_2O or diamond-zincblende structures,^{19,20} but it is also softer than the nearest-neighbor bonds of other NTE compounds, like Cu_2O , CuScO_2 ¹⁹ or even better ZrW_2O_8 .^{17a} Therefore, the stiffness of the Sc–F bond does not seem to be the only important factor in NTE.

From the comparison between thermal expansion of chemical bonds obtained by EXAFS and crystallographic thermal expansion by XRD, we can also estimate the MSRD perpendicular to bond directions.²¹ As shown in Figure 3b, the perpendicular MSRD_{\perp} of the Sc–F bond reveals a very large sensitivity to the temperature. It means that the transverse thermal vibration of fluorine is extremely large, as predicted by theory,²² and it will play a critical role in the NTE mechanism of ScF_3 . The corresponding effective “bond-bending” force constant k_{\perp} is 0.94(4) $\text{eV}/\text{Å}^2$, approximately 10× smaller than

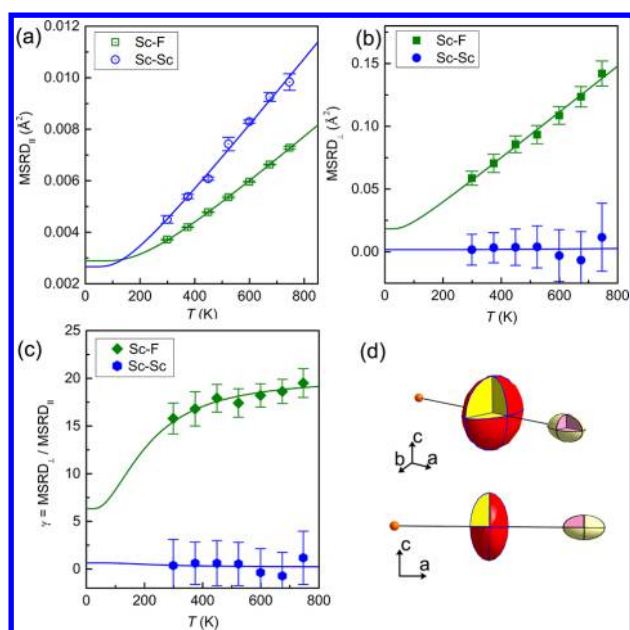


Figure 3. Atomic MSRDR of ScF_3 : (a) MSRDR_{\parallel} (parallel), (b) MSRDR_{\perp} (perpendicular), and (c) anisotropy of the relative thermal vibrations of the Sc–F and Sc–Sc atomic pairs determined by EXAFS. The lines are the best fitting Einstein models. (d) Schematic representation of the thermal ellipsoids of the relative thermal vibrations. The larger ellipsoid refers to the Sc–F relative motion and the smaller one to the Sc–Sc relative motion.

the stretching one. Accordingly, the Sc–F bond is much stiffer to stretch than to bend, and this could be related to the presence of empty space in the cubic ScF_3 structure perpendicularly to the Sc–F–Sc linkage. Contrarily, the perpendicular MSRDR_⊥ between the second-neighbors Sc–Sc is small and almost unchanged over the whole temperature range (Figure 3b).

From the ratio $\gamma = \text{MSRDR}_{\perp}/\text{MSRDR}_{\parallel}$ (Figure 3c) we can determine the anisotropy of the relative thermal vibrations. For perfect isotropy, $\gamma = 2$. It is interesting to observe that the γ ratio for the Sc–F bond is highly sensitive to the temperature and, above all, is large at high temperature where $\gamma \cong 20$. This value of γ is much larger than that of other NTE compounds, such as $\gamma = 6$ for Ge and Cu_2O and $\gamma = 11$ for CuCl , but is similar to $\gamma = 22$ of Ag_2O^{23} or $\gamma = 26\text{--}32$ of bridging oxygens of ZrW_2O_8 .^{17a} The larger values of γ could be related to the fact that in ScF_3 , Ag_2O and ZrW_2O_8 , contrary to Ge, Cu_2O , and CuCl , the NTE persists up to high temperatures. Turning to the Sc–Sc pair, however, the γ remains at low values and fairly stable over the whole temperature range. The value of γ is slightly smaller than 2, indicating that the Sc–Sc relative motion is more pronounced along the bond direction. Here, the thermal ellipsoids of the Sc–F and Sc–Sc relative thermal vibrations can be visualized by the schematic representation of Figure 3d. This figure gives evidence of the large transverse vibration of fluorine atoms normal to the Sc–F–Sc chain as well as that of the nearest-neighboring scandium atoms that are pulled closer together.

These experimental results demonstrate that the local vibrational dynamics for ScF_3 can be directly ascribed to the so-called “guitar-string” effect,^{17a,24} in which the bonds between some atomic pairs are so strong that the relative motion of the atoms along the bond direction is inhibited and the transverse motion to the bond direction is favorite. In the specific case of

ScF_3 , when the fluorine atom in the middle Sc–F–Sc linkage is displaced transversely, the Sc–F bonds tend to pull the two Sc atoms together thus inducing a pronounced NTE. It is important to highlight that this mechanism is firmly supported by ab initio MD and frozen phonon calculations.²² The dynamic transverse motion of fluorine atoms has a good agreement with the previous MD simulations, and this dynamic vibration of fluorine atoms correlates closely with quartic anharmonicity, contributing principally to NTE of ScF_3 .

It is also worth noting that the EXAFS parallel and perpendicular MSRDRs include only the dynamic contribution of the relative Sc–F and Sc–Sc motion. Even if a static contribution was present as the disorder structure model claims, this is proved from the MSRDRs.

In summary, this study provides new insight into the local dynamics of ScF_3 , one of the most recent and interesting NTE materials, by using X-ray total scattering EXAFS and NPD techniques. A considerable PTE of the true Sc–F bond distance and large transverse vibrations of fluorine atoms, perpendicular to the Sc–F–Sc linkage, has been observed, thus indicating that the Sc–F bond is much softer to bend than to stretch. Concomitantly, the true Sc–Sc distance shrinks, and the Sc–Sc relative motion is more pronounced along the bond direction. Besides, dynamic transverse motion of fluorine atoms is confirmed by Retveld analysis of high-resolution NPD data. The combination of these findings reveals the presence of a “guitar-string” effect as the local mechanism responsible for the NTE in ScF_3 .

■ ASSOCIATED CONTENT

📄 Supporting Information

The Supporting Information is available free of charge on the ACS Publications website at DOI: 10.1021/jacs.6b02370.

Sample preparation, experimental methods and data analysis procedures (PDF)

■ AUTHOR INFORMATION

Corresponding Authors

*junchen@ustb.edu.cn

*xing@ustb.edu.cn

Notes

The authors declare no competing financial interest.

■ ACKNOWLEDGMENTS

This work was supported by the National Natural Science Foundation of China (grant nos. 21322102, 91422301, 21231001, and 21590793), the Changjiang Young Scholars Award, National Program for Support of Top-notch Young Professionals, the Fundamental Research Funds for the Central Universities, China (FRF-TP-14-012C1). The use of the Advanced Photon Source at Argonne National Laboratory was supported by the U.S. Department of Energy, Office of Science, Office of Basic Energy Sciences (DE-AC02-06CH11357). We acknowledge the ELETTRA Synchrotron Radiation Facility for provision of synchrotron radiation as well as all the staff of the XAFS beamline. This work has been partially supported by the ELETTRA project no. 20140214.

■ REFERENCES

- (1) Mary, T. A.; Evans, J. S. O.; Vogt, T.; Sleight, A. W. *Science* **1996**, *272*, 90.
- (2) Mohn, P. *Nature* **1999**, *400*, 18.

- (3) Takenaka, K.; Takagi, H. *Appl. Phys. Lett.* **2005**, *87*, 261902.
- (4) Greve, B. K.; Martin, K. L.; Lee, P. L.; Chupas, P. J.; Chapman, K. W.; Wilkinson, A. P. *J. Am. Chem. Soc.* **2010**, *132*, 15496.
- (5) Hu, L.; Chen, J.; Fan, L.; Ren, Y.; Rong, Y.; Pan, Z.; Deng, J.; Yu, R.; Xing, X. *J. Am. Chem. Soc.* **2014**, *136*, 13566.
- (6) Evans, J. S. *J. Chem. Soc., Dalton Trans.* **1999**, *19*, 3317.
- (7) Chen, J.; Hu, L.; Deng, J.; Xing, X. *Chem. Soc. Rev.* **2015**, *44*, 3522.
- (8) (a) Goodwin, A. L.; Calleja, M.; Conterio, M. J.; Dove, M. T.; Evans, J. S.; Keen, D. A.; Peters, L.; Tucker, M. G. *Science* **2008**, *319*, 794. (b) Goodwin, A. L.; Kepert, C. J. *Phys. Rev. B: Condens. Matter Mater. Phys.* **2005**, *71*, 140301. (c) Chapman, K. W.; Chupas, P. J.; Kepert, C. J. *J. Am. Chem. Soc.* **2005**, *127*, 15630.
- (9) (a) Zheng, X. G.; Kubozono, H.; Yamada, H.; Kato, K.; Ishiwata, Y.; Xu, C. N. *Nat. Nanotechnol.* **2008**, *3*, 724. (b) Huang, R. J.; Liu, Y.; Fan, W.; Tan, J.; Xiao, F.; Qian, L.; Li, L. F. *J. Am. Chem. Soc.* **2013**, *135*, 11469. (c) Zhao, Y. Y.; Hu, F. X.; Bao, L. F.; Wang, J.; Wu, H.; Huang, Q. Z.; Wu, R.; Liu, Y.; Shen, F.; Kuang, H.; Zhang, M.; Zuo, W.; Zheng, X.; Sun, J.; Shen, B.-G. *J. Am. Chem. Soc.* **2015**, *137*, 1746. (d) Chen, J.; Nittala, K.; Forrester, J. S.; Jones, J. L.; Deng, J.; Yu, R.; Xing, X. *J. Am. Chem. Soc.* **2011**, *133*, 11114.
- (10) Azuma, M.; Chen, W. T.; Seki, H.; Czapski, M.; Oka, K.; Mizumaki, M.; Attfield, J. P. *Nat. Commun.* **2011**, *2*, 347.
- (11) Tallentire, S. E.; Child, F.; Fall, I.; Vella-Zarb, L.; Evans, I. R.; Tucker, M. G.; Keen, D. A.; Wilson, C.; Evans, J. S. *J. Am. Chem. Soc.* **2013**, *135*, 12849.
- (12) Attfield, J. P. *Nature* **2011**, *480*, 465.
- (13) (a) Wu, Y.; Kobayashi, A.; Halder, G. J.; Peterson, V. K.; Chapman, K. W.; Lock, N.; Kepert, C. J. *Angew. Chem.* **2008**, *120*, 9061. (b) Han, S. S.; Goddard, W. A. *J. Phys. Chem. C* **2007**, *111*, 15185.
- (14) Tao, J. Z.; Sleight, A. W. *J. Solid State Chem.* **2003**, *173*, 442.
- (15) Tucker, M. G.; Goodwin, A. L.; Dove, M. T.; Keen, D. A.; Wells, S. A.; Evans, J. S. O. *Phys. Rev. Lett.* **2005**, *95*, 255501.
- (16) (a) Cao, D.; Bridges, F.; Kowach, G. R.; Ramirez, A. P. *Phys. Rev. Lett.* **2002**, *89*, 215902. (b) Bridges, F.; Keiber, T.; Juhas, P.; Billinge, S. J. L.; Sutton, L.; Wilde, J.; Kowach, G. R. *Phys. Rev. Lett.* **2014**, *112*, 045505.
- (17) (a) Sanson, A. *Chem. Mater.* **2014**, *26*, 3716. (b) Lazar, P.; Bučko, T.; Hafner, J. *Phys. Rev. B: Condens. Matter Mater. Phys.* **2015**, *92*, 224302.
- (18) (a) Dalba, G.; Fornasini, P. *J. Synchrotron Radiat.* **1997**, *4*, 243. (b) Fornasini, P.; Grisenti, R. *J. Synchrotron Radiat.* **2015**, *22*, 1242.
- (19) Ahmed, S. I.; Dalba, G.; Fornasini, P.; Vaccari, M.; Rocca, F.; Sanson, A.; Sleight, A. W. *Phys. Rev. B: Condens. Matter Mater. Phys.* **2009**, *79*, 104302.
- (20) Abd el All, N.; Dalba, G.; Diop, D.; Fornasini, P.; Grisenti, R.; Mathon, O.; Rocca, F.; Sendja, B. T.; Vaccari, M. *J. Phys.: Condens. Matter* **2012**, *24*, 115403.
- (21) Fornasini, P.; a Beccara, S.; Dalba, G.; Grisenti, R.; Sanson, A.; Vaccari, M.; Rocca, F. *Phys. Rev. B: Condens. Matter Mater. Phys.* **2004**, *70*, 174301.
- (22) Li, C. W.; Tang, X.; Muñoz, J. A.; Keith, J. B.; Tracy, S. J.; Abernathy, D. L.; Fultz, B. *Phys. Rev. Lett.* **2011**, *107*, 195504.
- (23) Vaccari, M.; Grisenti, R.; Fornasini, P.; Rocca, F.; Sanson, A. *Phys. Rev. B: Condens. Matter Mater. Phys.* **2007**, *75*, 184307.
- (24) Barrera, G. D.; Bruno, J. A. O.; Barron, T. H. K.; Allan, N. L. *J. Phys.: Condens. Matter* **2005**, *17*, R217.